

Two-atom resonant radiative coupling in photonic band structures

Gershon Kurizki

Department of Chemical Physics, Weizmann Institute of Science, Rehovot 76100, Israel

(Received 6 April 1990)

Radiative coupling between identical atoms sharing an excitation is studied in media where dispersion creates photonic band gaps, i.e., forbidden bands of light propagation for all directions and polarizations. Photonic band gaps can exist in media whose dielectric index exhibits strong three-dimensionally periodic modulations ("photonic crystals") or in bands of polaritonic media. It is shown that the resonant dipole-dipole interaction as well as cooperative fluorescence of two-atom systems can be strongly enhanced or suppressed, to the extent of being essentially eliminated, by one of the following mechanisms: (a) dependence on location of the atoms within a unit cell of a photonic crystal, i.e., sensitivity to the spatial variation of the field normal modes; (b) dependence on the density of normal modes in allowed bands and on the density of virtual (evanescent) modes in band gaps. The ability to suppress the dipole-dipole interactions at interatomic separations characterizing quasimolecules would have far-reaching implications on their dissociative or collisional dynamics, spectroscopy, and rates of energy transfer.

I. INTRODUCTION

Two identical atoms sharing an excitation are coupled by a resonant radiative interaction (self-energy) whose imaginary part expresses the change in the rate of atomic radiative decay while the real part corresponds to a spectral shift, known as the resonant dipole-dipole interaction (RDDI).^{1,2} In free space the RDDI between atoms with transition frequency ω_0 and dipole moment μ attains the electrostatic limit $\sim \mu^2/\hbar R^3$ at separations R much shorter than the emission wavelength. This short-range limit of the RDDI is largely responsible for the spectra, energy transfer rates, and dynamics of electronically excited diatoms or molecular dimers in bound states^{3,4} or during collisions^{5,6} and dissociation,⁷ as well as for dephasing in multiatomic cooperative emission.⁸ It is therefore of conceptual and phenomenological import to study modifications of the free-space interatomic radiative coupling by the medium containing the atoms, which can either enhance or suppress the RDDI relative to its electrostatic short-range limit.

Until recently, little effort has been made to address such questions, in contrast to thorough studies of modified fluorescence and Lamb shift properties of a single atom near a surface (mirror) (Refs. 9 and 10) or in a resonator (two parallel mirrors).¹¹⁻¹³ Yet recent works have indicated that the electrostatic free-space limit of the RDDI is by no means an immutable property: (a) RDDI enhancement at small separations has been demonstrated for molecules in a dielectric microsphere, when a dipolar transition frequency coincides with a Mie scattering resonance.^{14,15} (b) The possibility of RDDI suppression has been suggested¹⁶ for dipolar transitions within a photonic band gap, i.e., a spectral band of forbidden dispersion where the density of propagating photon modes vanishes for all directions and polarizations.

A photonic band gap has been originally conceived¹⁷ to

be an environment where spontaneous emission at a chosen frequency is extinguished by the vanishing of the density of modes (DOM) at that frequency. This vanishing is a spatially invariant property, which should affect radiatively coupled atoms independently of their location, in contrast to modifications of radiative properties in previously considered structures (surfaces, resonators, or microparticles) where atomic location plays a crucial role.⁹⁻¹⁵ A photonic band gap therefore promises to be a unique type of environment of field-matter interactions, which merits detailed investigations. Photonic band gaps can be studied in the following wide range of media combining the requirement of forbidden dispersion with that of weak dissipation (since dissipative effects spoil band-gap properties, as shown here).

a. Photonic crystals. It has been proposed¹⁷ that structures whose dielectric index exhibits strong three-dimensionally periodic modulations can have a photonic band gap at wavelengths that are roughly twice the modulation period. Photonic crystals are also candidates for strong localization of light at frequencies near the band gap edge in the presence of some disorder.¹⁸ Anomalous Lamb shifts are predicted for atomic transitions near band gaps.¹⁹ A photonic crystal with a band gap at microwave frequencies has already been realized,²⁰ and it should be possible to obtain band gaps at infrared or optical wavelengths using analogous structures: superlattices,¹⁷ colloidal crystals, or three-dimensional optical gratings saturating near-resonant media.²¹

b. Anomalous Dispersive Nearly Uniform Media. Band gaps arise in many isotropic materials at frequencies between the pole and zero of their frequency-dependent dielectric index associated with polaritonic dispersion.²² "Optically-dressed" phonons give rise to polaritonic band gaps in the infrared region,^{23,24} while saturated two-photon biexcitonic transitions (e.g., in CuCl) produce polaritonic band gaps in the visible or near-

ultraviolet region.²⁵ Another type of forbidden band is found below the cutoff frequency of the medium in metal plasmas (typically in the ultraviolet region) or in microwave waveguides.

This paper is aimed at providing a more comprehensive understanding of radiative coupling between atoms whose transition frequencies lie within or near photonic band gaps. The present treatment is based on the assumption that the dispersion is isotropic, which can be accurate for band gaps in nearly uniform media but is only qualitatively applicable to photonic crystals. The general analysis (Sec. II) shows that the interatomic radiative coupling depends on the modified DOM, but, in photonic crystals, is also sensitive to atomic location within a unit cell. This result allows us to elucidate the connection between the radiative effects of photonic crystals and those of resonators or microparticles. Section III describes the modified radiative coupling in allowed bands, including band tails occurring in partly disordered photonic crystals, where the DOM function can nearly vanish but remains smooth (analytic) at all frequencies. Sec. IV considers the effects of the abrupt, singular vanishing of the DOM function at band gap edges in perfect photonic crystals or lossless polaritonic media. Striking differences are found between the RDDI behavior in band gaps and band tails, yet strong suppression of RDDI and fluorescence rates occurs in both cases. Dissipative effects are shown to bridge between these two types of suppression. (Sec. IV). The implications of RDDI and fluorescence suppression on the temporal evolution of diatoms and donor-acceptor energy transfer are discussed in Sec. V.

II. GENERAL ANALYSIS

A. Self-energy expansion in normal modes

We consider two atoms located at points \mathbf{r}_A , and \mathbf{r}_B in a dispersive medium and sharing an excitation at a transition with dipole moment $\boldsymbol{\mu}$ and frequency ω_0 . The interatomic interaction (two-atom self-energy) is associated with cross products of the dipole coupling to the vacuum field¹ at the two atomic positions and times t, t'

$$\langle \text{vac} | \boldsymbol{\mu} \cdot \mathbf{E}(\mathbf{r}_A, t) \boldsymbol{\mu} \cdot \mathbf{E}(\mathbf{r}_B, t') | \text{vac} \rangle$$

and therefore expresses the interference between the emission and absorption of a photon by the two atoms.

In free space the field is conveniently expanded in terms of plane waves with wave vectors \mathbf{k} and frequencies ck , whence the foregoing cross products are written as \mathbf{k} sums of the interference factors^{1,26} $(\boldsymbol{\mu} \cdot \hat{\boldsymbol{\eta}}_\sigma)^2 \exp(i\mathbf{k} \cdot \mathbf{R})$, where $\hat{\boldsymbol{\eta}}_\sigma$ is a unit vector of polarization and $\mathbf{R} = \mathbf{r}_A - \mathbf{r}_B$. The general prescription used here is the expansion of the field in normal modes of the medium

$$\mathbf{E}(\mathbf{r}) = \sum_{\alpha=\mathbf{K}, n, \sigma} \hat{\boldsymbol{\eta}}_\sigma (2\pi\omega_\alpha/V)^{1/2} \psi_\alpha(\mathbf{r}) a_\alpha + \text{H.c.}, \quad (1)$$

where ω_α , ψ_α , and a_α denote the mode frequency, spatial envelope (mode function), and annihilation operator, respectively, and V is the quantization volume. The mode functions $\psi_\alpha(\mathbf{r})$ incorporate the boundary conditions and

dispersive properties of the medium.

In structures with three-dimensional periodicity the dielectric index $\epsilon(\mathbf{r})$ can be expanded as a Fourier series in reciprocal-lattice vectors \mathbf{g} ,

$$\epsilon(\mathbf{r}) = \sum_{\mathbf{g}} \epsilon_{\mathbf{g}} e^{i\mathbf{g} \cdot \mathbf{r}}. \quad (2a)$$

The shortest $\mathbf{g} \neq 0$ in this expansion can have the length $2\pi/d$, d being the shortest structure period. The appropriate mode functions are labeled by their quasi-momentum $\hbar\mathbf{K}$, which is restricted to the first Brillouin zone $|\mathbf{K}| \leq \pi/d$, band index n , and polarization σ :

$$\psi_\alpha(\mathbf{r}) = e^{i\mathbf{K} \cdot \mathbf{r}} \sum_{\mathbf{g}} C_{\mathbf{g}\alpha} e^{i\mathbf{g} \cdot \mathbf{r}}. \quad (2b)$$

Band gaps arise in such structures when the vectorial wave equation for $\mathbf{E}(\mathbf{r}\omega_\alpha)$ near the edge of the Brillouin zone $|\mathbf{K}| \simeq \pi/d$ has only complex \mathbf{K} solutions for all directions and polarizations^{18,27} [Fig. 1(a)].

In isotropic ionic crystals, field propagation with frequencies near phonon resonances is described by polariton modes, which are plane waves labeled, for each wave vector \mathbf{K} , by a branch index $n = \pm$ of the approximate dispersion relation^{23,24}

$$c^2 \mathbf{K}^2 / \omega^2 = \epsilon(\omega) = \epsilon_0 + \Omega_p^2 / (\omega_T^2 - \omega^2) \quad (3a)$$

where ϵ_0 is the nonresonant dielectric index, Ω_p^2 is an effective plasma frequency of the ionic lattice, and ω_T is the transverse optical phonon frequency. The region between the (far-infrared) frequencies of transverse and longitudinal optical phonons ω_T and ω_L

$$\omega_T \leq \omega \leq \omega_L = [(\omega_T^2 + \Omega_p^2 / \epsilon_0)^{1/2}] \quad (3b)$$

corresponds to $\epsilon(\omega) < 0$ and is therefore a band gap, where propagating field modes are forbidden. A more complicated but essentially analogous polaritonic dispersion and band gap are exhibited by isotropic semiconduc-

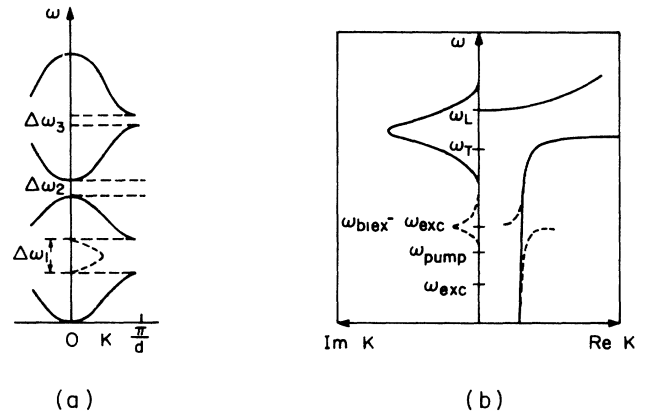


FIG. 1. Dispersion and bandgaps in (a) periodic media and (b) media with induced polaritonic dispersion, e.g., CuCl. In (a) the gaps occur at the Bragg resonance $K = \pi/d$, and $\text{Im}K$ in the gap is denoted by the dashed curve. In (b) the gap occurs between ω_T and ω_L in the presence of pump saturation near $\omega_{\text{biox}} - \omega_{\text{exc}}$ where ω_{biox} and ω_{exc} are the biexcitonic and excitonic transitions.

tors in the presence of a saturating optical pump, near half the frequency of their biexcitonic transition (3.185 eV in CuCl) (Ref. 25) [Fig. 1(b)].

A third type of normal mode that will be considered here is the transverse mode of field propagation in electronic plasmas. The medium is transparent above the plasma frequency ω_p (a few electron volts in alkali metals), where the dielectric index is

$$\epsilon(\omega) = 1 - \omega_p^2 / \omega^2 \quad (4)$$

and has a cutoff at $\omega = \omega_p$, below which $\epsilon(\omega) < 0$. Microwave waveguides behave analogously.

On adapting the prescriptions of Lehmborg²⁶ or Agarwal² to the normal-mode basis, the time-dependent self-energy can be written as follows, on separating its real and imaginary parts:

$$\begin{aligned} -i\Omega^{AB} + \gamma^{AB} = & (2\pi/V) \sum_{\alpha} \omega_{\alpha} \psi_{\alpha}^*(\mathbf{r}_A) \psi_{\alpha}(\mathbf{r}_B) (\boldsymbol{\mu} \cdot \hat{\boldsymbol{\eta}}_{\sigma})^2 \\ & \times \left[\frac{1 - \cos(\omega_{\alpha} - \omega_0)t}{i(\omega_{\alpha} - \omega_0)} \right. \\ & \left. + \frac{\sin(\omega_{\alpha} - \omega_0)t}{\omega_{\alpha} - \omega_0} \right] \\ & + (\omega_0 \rightarrow -\omega_0), \end{aligned} \quad (5)$$

where the last term has the same form as the first one, but with ω_0 replaced by $-\omega_0$. For long times compared to an optical period ($\omega_0 t \gg 1$) and moderate retardation [which is ensured in our case, since we wish to consider $K(\omega_0)R \lesssim 1$, $\omega_0 R/c \lesssim 1$] we can take the Markovian limit of Eq. (5):

$$\begin{aligned} -i\Omega^{AB} + \gamma^{AB} = & (2\pi/V) \sum_{\alpha} \omega_{\alpha} \psi_{\alpha}^*(\mathbf{r}_A) \psi_{\alpha}(\mathbf{r}_B) (\boldsymbol{\mu} \cdot \hat{\boldsymbol{\eta}}_{\sigma})^2 \\ & \times \left[-iP \left[\frac{1}{\omega_{\alpha} - \omega_0} + \frac{1}{\omega_{\alpha} + \omega_0} \right] \right. \\ & \left. + \pi \delta(\omega_{\alpha} - \omega_0) \right]. \end{aligned} \quad (6)$$

The principal-value (P) term Ω_{AB} is recognized to be the RDDI shift, whereas the δ -function term γ^{AB} is the cooperative change of the atomic rate of fluorescence.

The Markovian limit is equivalent to the pole approximation,^{2,28} in which one neglects shifts from the difference between mode and resonance frequencies $\omega_{\alpha} \mp \omega_0$. This approximation assumes that the modes constitute a continuum, so that any reasonable pole shift is replaceable by a mode frequency ω_{α} . Such a continuum causes irreversible decay of excited states. Equation (6) is then evaluated in the limit

$$\sum_{\alpha=\mathbf{K},n,\sigma} \longrightarrow V \sum_{n,\sigma} \int d\Omega_{\hat{\mathbf{K}}} \int K^2 dK \quad (7)$$

with $\int d\Omega_{\hat{\mathbf{K}}}$ denoting solid-angle integration and $\int K^2 dK$ extending over the first Brillouin zone (in periodic media) or a single polariton branch.

B. Directional integrals in the isotropic approximation

The next assumption to be made here is the strongest restriction on the present treatment, namely, that of isotropic dispersion, in which ω depends only on the modulus of \mathbf{K} . This assumption is accurate for isotropic, nearly uniform media with polaritonic or plasma dispersion. It can also be invoked in periodically modulated media (photonic crystals), as is commonly done for electron or phonon bands in natural crystals,^{29,30} approximating the polyhedral Brillouin surface in \mathbf{K} space by a sphere. In the photonic (microwave) fcc crystal recently fabricated by Yablonovitch²⁰ the band gap width normalized to the frequency of the band center is $\sim \frac{1}{4}$ in the L direction of the Brillouin surface and only $\sim \frac{1}{10}$ in the X direction. The isotropic approximation, which implies the replacement of these widths by a directionally averaged width is then rather crude, yet it is qualitatively valid as long as the gap width is non-negligible in all directions. This approximation is obviously inadequate in strongly anisotropic media where the alignment of molecular dipoles with inequivalent symmetry axes leads to the splitting of RDDI shifts known as the Davydov splitting.³¹ Likewise, it fails for atoms located between two mirrors, whose mirror images form a one-dimensional lattice whereas the DOM in the mirror planes is that of free space.^{12,13}

The evaluation of Ω^{AB} and γ^{AB} in the foregoing approximations first requires the performance of angular integration over the terms of Eq. (6). This integral has the following form for plane wave ψ_{α} and dimer states with $\boldsymbol{\mu} \parallel \mathbf{R}$ (Σ states) or $\boldsymbol{\mu} \perp \mathbf{R}$ (Π states)

$$\begin{aligned} & \int d\Omega_{\hat{\mathbf{K}}} (\hat{\boldsymbol{\mu}} \cdot \hat{\boldsymbol{\eta}}_{\sigma})^2 \psi_{\alpha}^*(\mathbf{r}_A) \psi_{\alpha}(\mathbf{r}_B) \\ & = \frac{1}{2} \int d\Omega_{\hat{\mathbf{K}}} [1 - (\hat{\boldsymbol{\mu}} \cdot \hat{\mathbf{K}})^2] \exp(i\mathbf{K} \cdot \mathbf{R}) \\ & \equiv F(KR) \end{aligned} \quad (8a)$$

where $\hat{\boldsymbol{\mu}}$ denotes the unit vector along $\boldsymbol{\mu}$. Explicitly²⁶

$$F_{\Sigma}(KR) = 3[\sin(KR)/(KR)^3 - \cos(KR)/(KR)^2], \quad (8b)$$

$$\begin{aligned} F_{\Pi}(KR) = & -\frac{3}{2}[\sin(KR)/(KR)^3 - \cos(KR)/(KR)^2 \\ & - \sin(KR)/KR]. \end{aligned} \quad (8c)$$

The generalization of Eqs. (8) to Bloch waves (2b) yields, on ignoring the dependence of $C_{g\alpha}$ on the direction of \mathbf{K} (consistently with the isotropic approximation)

$$\int d\Omega_{\hat{\mathbf{K}}} (\hat{\boldsymbol{\mu}} \cdot \hat{\boldsymbol{\eta}}_{\sigma})^2 \langle \psi_{\alpha}^*(\mathbf{r}_A) \psi_{\alpha}(\mathbf{r}_B) \rangle = \frac{1}{2} F(KR) \Phi_{\alpha}^{AB}, \quad (9a)$$

where the angular brackets denote averaging over the orientations of \mathbf{R} and $\mathbf{r}_{A(B)}$ and

$$\Phi_{\alpha}^{AB} = 2 \sum_{\mathbf{g}} \frac{\sin(\mathbf{g}R)}{gR} \left[|C_{\mathbf{g}\alpha}|^2 + \sum_{\mathbf{g}'(\mathbf{g}' \neq \mathbf{g})} C_{\mathbf{g}\alpha}^* C_{\mathbf{g}'\alpha} \frac{\sin(|\mathbf{g}-\mathbf{g}'|r_B)}{|\mathbf{g}'-\mathbf{g}|r_B} \right] \quad (9b)$$

expresses the effects of lattice diffraction. Note that in general $\Phi_{\alpha}^{AB} \neq \Phi_{\alpha}^{BA}$ because r_A and r_B are not necessarily symmetric with respect to the origin $r=0$ of the unit cell. This origin is arbitrarily positioned, but, since this choice determines the $C_{\mathbf{g}\alpha}$'s, it is convenient to place it at a peak or trough of $\epsilon(\mathbf{r})$. An analogous dependence of radiative properties on location within the unit cell is found for an atom between two mirrors,^{12,13} whose spacing is the unit cell of the one-dimensional lattice of image atoms.

The form of Φ_{α}^{AB} in (9b) is convenient when the atoms are located in spatial regions where the modulation of $\epsilon(\mathbf{r})$ in (2a) is moderate and nearly sinusoidal, allowing us to retain only a few \mathbf{g} and \mathbf{g}' contributions (See III). However, when the atoms are located within or on spheres whose dielectric index is strongly different from that of the surrounding, as in the Yablonovitch muffin-tin

crystal,²⁰ then an altogether different approximation is called for. Although the KKR (Korringa-Kohn-Rostoker) approximation is better suited for band structure calculations in muffin-tin structures,^{30,32} the wave functions have a more transparent form in the augmented-plane-wave (APW) approximation.^{29,30} In this approximation, each plane-wave component of the Bloch wave $C_{\mathbf{g}\alpha} e^{-i(\mathbf{K}-\mathbf{g})\cdot\mathbf{r}}$ outside the spheres is matched with the single-sphere solution of the wave equation at the surface of a sphere which is centered at a point \mathbf{r}_j in the unit cell. The equivalent of Eqs. (9) can be written for \mathbf{r}_A and \mathbf{r}_B located near the spheres at \mathbf{r}_j and $\mathbf{r}_{j'}$, on averaging over the atomic angular positions relative to the spheres. This averaging allows the elimination of cross terms of electric and magnetic multipoles of different spherical harmonics.¹⁴ The result is

$$F(KR)\Phi_{\alpha}^{AB} \longrightarrow F(K|\mathbf{r}_j - \mathbf{r}_{j'}|)\Phi_{\alpha}^{jj'} \\ \times \sum_{n,l,m} \left[|C_{nlm}^{(M)}|^2 j_l(k_s R_A) j_l(k_s R_B) + |C_{nlm}^{(E)}|^2 \left[\frac{l}{2l+1} j_{l+1}(k_s R_A) j_{l+1}(k_s R_B) \right. \right. \\ \left. \left. + \frac{l+1}{2l+1} j_l(k_s R_A) j_{l-1}(k_s R_B) \right] \right]. \quad (10)$$

Here $\Phi_{\alpha}^{jj'}$ has the same form as (9b), but with r_A, r_B replaced by $r_j, r_{j'}$. Also, $k_s = (\omega_{\alpha}/c)\epsilon_s^{1/2}$, ϵ_s being the dielectric index of the sphere, $R_A = |\mathbf{r}_A - \mathbf{r}_j|$, $R_B = |\mathbf{r}_B - \mathbf{r}_{j'}|$, and $C_{nlm}^{(M)}$ and $C_{nlm}^{(E)}$ are magnetic and electric multipole contributions, respectively, of the single-sphere field expansions which are determined by matching to the plane wave outside the sphere. It is obvious that for atoms within the same sphere the coupling will mainly be sensitive to the field variation within the sphere, whereas for atoms located near or at different spheres the spherical field variation will be modulated by the same diffraction factors as in Eqs. (9) [Fig. 2(a)]. This reveals the strong dependence of the coupling on the radial positions of the atoms and the radii R_s of the spheres themselves. If the Mie resonance condition is satisfied within a sphere (this requires $\epsilon_s \gg 1$ and close packing, so that $k_s R_s \gtrsim 2\pi$), then certain $C_{nlm}^{(E)}$ or $C_{nlm}^{(M)}$ in Eq. (10) become enormously enhanced compared to others. The interatomic coupling would then exhibit an enhancement of the type that has been demonstrated in a single sphere,^{14,15} yet $F(K|\mathbf{r}_j - \mathbf{r}_{j'}|)\Phi_{\alpha}^{jj'}$ would impose periodic structural modifications on the Mie-type enhancement. Thus, the Mie-resonant field would be strongly diminished when the appropriate Bloch wave has a node at one or both of the atomic locations [Fig. 2(a)].

C. Generalized expressions for two-atom coupling

The final step towards obtaining the general expressions for Ω^{AB} and γ^{AB} in the considered media involves the conversion of $K^2 dK$ in Eq. (7) into the frequency-space density of modes:

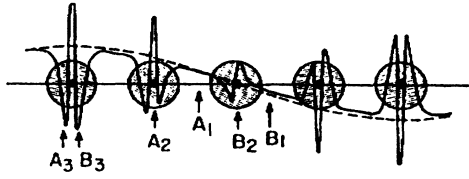
$$N_n(\omega) = \frac{1}{2} \sum_{\sigma=1,2} \left[K^2(\omega) \left| \frac{dK}{d\omega} \right| \right]_{n\sigma} \quad (11)$$

where the sum is over polarizations and $|K|$ is a well-defined function of $|\omega|$, and vice versa, in the $n\sigma$ band (this point will be further discussed in Secs. III and IV).

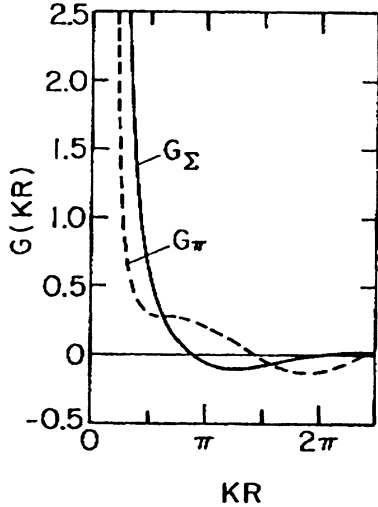
It is now possible to write the self-energy expressions in their final form, using Eqs. (7)–(9), and normalizing them by their free-space counterparts:

$$\frac{\gamma^{AB}(\omega_0, \mathbf{R}, \mathbf{r}_j)}{\gamma_{\text{free}}^{AB}(\omega_0, \mathbf{R})} = \frac{c^3 N_n(\omega_0) [F(KR)\Phi^{AB}]_{n\omega_0}}{F(\omega_0 R/c)}, \quad (12)$$

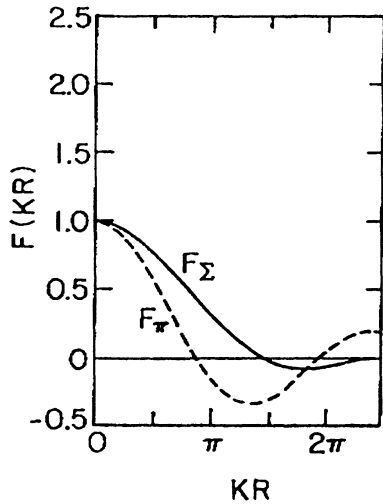
$$\frac{\Omega^{AB}(\omega_0, \mathbf{R}, \mathbf{r}_j)}{\Omega_{\text{free}}^{AB}(\omega_0, \mathbf{R})} \\ = \frac{c^3}{\omega_0^3 G(\omega_0 R/c)} \sum_n P \int d\omega \frac{N_n(\omega) \omega^2 [F(KR)\Phi^{AB}]_{n\omega}}{\omega^2 - \omega_0^2}. \quad (13)$$



(a)



(b)



(c)

FIG. 2. (a) Spatial dependence of the field normal modes which couple pairs of atoms in periodic arrays of spheres. Atoms A_1 and B_1 "feel" the variation of a Bloch wave in the cell. A Bloch wave superimposed on Mie-resonant field variation couples atoms A_2 and B_2 in different spheres or A_3 and B_3 in the same sphere. (b) Separation dependence of the RDDI without crystal diffraction. (c) Same as (b) for the cooperative contribution to the decay rate.

Here, ω_0^2/c^3 is the free-space DOM, the summation of principal-value integrals in Eq. (13) extends over the band(s) and band gap adjacent to the ω_0 transition, and the free-space R dependence of Ω^{AB} is given by¹⁶

$$G_{\Sigma}(\omega_0 R/c) = i[F_{\Sigma}(+\omega_0 R/c) - F_{\Sigma}(-\omega_0 R/c)] \\ = -\frac{3}{2} \left[\frac{\cos(\omega_0 R/c)}{(\omega_0 R/c)^3} + \frac{\sin(\omega_0 R/c)}{(\omega_0 R/c)^2} \right] \quad (14)$$

or

$$G_{\Pi}(\omega_0 R/c) = i[F_{\Pi}(+\omega_0 R/c) - F_{\Pi}(-\omega_0 R/c)] \\ = \frac{3}{4} \left[\frac{\cos(\omega_0 R/c)}{(\omega_0 R/c)^3} + \frac{\sin(\omega_0 R/c)}{(\omega_0 R/c)^2} \right. \\ \left. - \frac{\cos(\omega_0 R/c)}{(\omega_0 R/c)} \right]. \quad (15)$$

We shall be mostly concerned with the short-separation limit $\omega_0 R/c \ll 1$ in which [Fig. 2(c)]

$$F_{\Sigma(\Pi)}(\omega_0 R/c) = \gamma_{\text{free}}^{AB}(\omega_0 R/c)/\gamma(\omega_0) \longrightarrow 1, \quad (16)$$

$\gamma(\omega_0)$ being the Einstein A coefficient, whereas $\Omega_{\text{free}}^{AB}(\omega_0, \mathbf{R})$ attains the electrostatic limit, as [Fig. 2(b)]

$$G_{\Sigma(\Pi)}(\omega_0 R/c) \longrightarrow (\omega_0 R/c)^{-3}. \quad (17)$$

On examining Eqs. (12) and (13) it is seen that the enhancement or suppression of γ^{AB} and Ω^{AB} by the medium is determined by the DOM modification factor $N_n(\omega)c^3/\omega^2$, the ratio cK/ω and the diffraction function Φ^{AB} (in crystals). All of these factors stem from *nonlocal* properties of the medium averaged over many optical cycles. Thus, in photonic crystals $N_n(\omega)$ and Φ_n^{AB} are both determined by Bragg reflections of the photon, which affect the interference between its emission and reabsorption by the coupled atoms.

III. ALLOWED BANDS AND BAND TAILS

A. General results

In this section we consider atomic transition frequencies ω_0 located within bands of allowed dispersion where the DOM function is analytic in the range contributing to RDDI. We thus avoid meanwhile the case of close proximity to a singularity of the DOM, e.g., a band edge in an ideal photonic crystal or a lossless polaritonic band [Figs. 3(a)–3(c)].

In addition to the analyticity of $N_n(\omega)$, we can make use of its even parity with respect to ω in isotropic, nearly uniform media and simple periodic structures (in both the nearly free and tight-binding regimes). The factors $[F(KR)\Phi^{AB}]_{\omega_n}$ are likewise even in ω in these media. These properties allow us to extend the integration limits to $\int_{-\infty}^{\infty} d\omega$, keeping the positive-frequency part of $F(KR)_{\omega_n}$ [Eqs. (8)] in the integrand. When K is an odd function of ω_n (nearly linear dispersion) this implies keep-

ing the complex, positive- K part of $F(KR)$, namely,

$$F_{\Sigma}(KR)_{+\omega n} = \frac{3}{2} \left[\frac{\exp(iKR)}{i(KR)^3} - \frac{\exp(iKR)}{(KR)^2} \right]_{\omega n} \quad (18)$$

and likewise for $F_{\Pi}(KR)_{+\omega n}$. If K is even in ω_n , then the entire $F(KR)$ function is retained in the integrand. In $ei-$

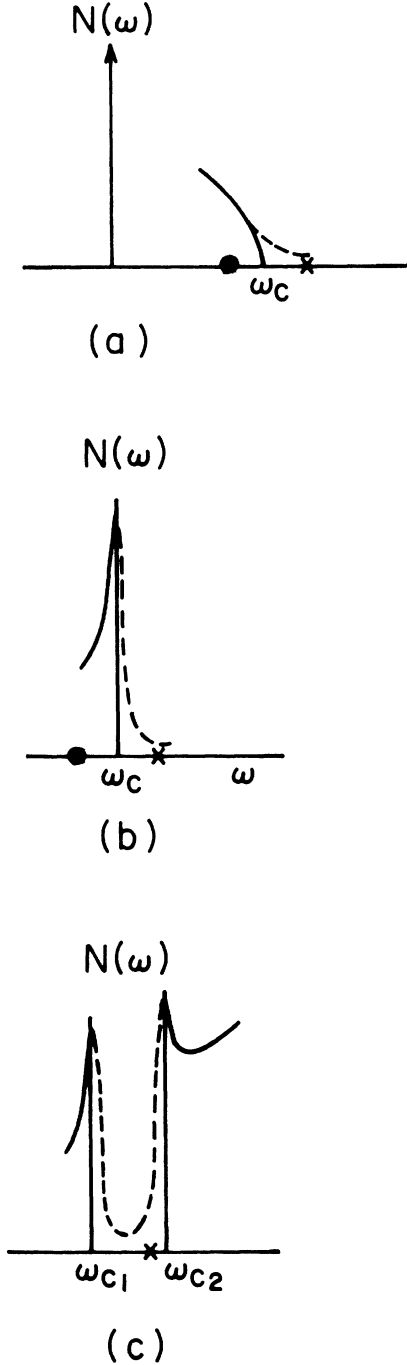


FIG. 3. The density of modes near the edge of a tightly bound band (a), near a cutoff (b) or near the gap between nearly free crystalline bands (c). The solid curves are modified into dashed curves in the presence of disorder, which smooths out the singularities. The dots mark locations of ω_0 in allowed bands and the crosses mark the ones in forbidden regions.

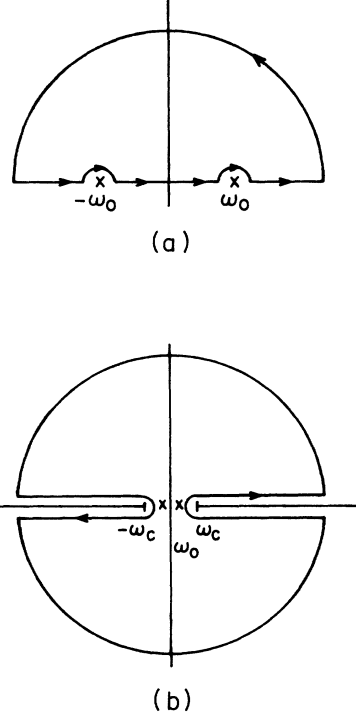


FIG. 4. Integration contours in the complex plane used in the evaluation of RDDI for ω_0 in (a) allowed bands or band tails and (b) below the cutoff [Fig. 3(b)].

ther case, integration along an infinite-radius semicircle in the upper half plane avoiding the poles $\omega = \pm\omega_0$ [Fig. 4(a)] and use of the residue theorem yield, by virtue of the parity of $N_n(\omega)$,

$$\begin{aligned} \Omega^{AB}(\omega_0, \mathbf{R}) / \Omega_{\text{free}}^{AB}(\omega_0, \mathbf{R}) \\ = [c^3 N_n(\omega_0) / \omega_0^2] [G(KR)_{\omega_0 n} / G(\omega_0 R / c)] \Phi_{\omega_0 n}^{AB}, \end{aligned} \quad (19)$$

where $G(KR)$ is given for Σ or Π states by Eqs. (14) or (15).

B. Nearly uniform media

The short-separation limit for the RDDI shift is seen from Eq. (19) to be of the same form as in free space, $\sim (KR)_{\omega_0}^{-3}$. However, when $\epsilon_n(\omega_0) \gg 1$, e.g., for ω_0 just below the polaritonic resonance ω_T [Eq. (3)], separations satisfying the electrostatic free-space limit $R \ll c/\omega_0$ can actually correspond to $(KR)_{\omega_0} = \epsilon_n^{1/2}(\omega_0)(\omega_0 R / c) \sim 1$, for which retardation effects are significant. The same is true for $\gamma^{AB}(\omega_0, \mathbf{R})$ [Eq. (12)], whose separation dependence is given by $F(KR)_{\omega_0 n}$. The most dramatic retardation effects would be, e.g., [Fig. 2(b)]

$$(KR)_{\omega_0} = -\cot(KR)_{\omega_0} \longrightarrow G_{\Sigma}(KR)_{\omega_0} = 0, \quad (20)$$

where Ω^{AB} vanishes irrespective of the DOM factor.

The DOM factor in Eqs. (12) and (19) can be written for allowed bands of nearly uniform media as

$$N_n(\omega_0) = (\omega_0^2/c^3)\epsilon_n^{3/2}(\omega_0) \left| 1 - \frac{\omega}{2} \frac{d}{d\omega} \ln \epsilon_n(\omega) \right|_{\omega_0}. \quad (21)$$

When the short-separation limit holds for both $\omega_0 R/c$ and $(KR)_{\omega_0}$, the use of this factor in Eq. (19) yields

$$\frac{\Omega^{AB}(\omega_0, \mathbf{R})}{\Omega_{\text{free}}^{AB}(\omega_0, \mathbf{R})} \simeq \frac{c}{|d\omega/dK|} = \left| 1 - \frac{\omega}{2} \frac{d}{d\omega} \ln \epsilon_n(\omega) \right|_{\omega_0}. \quad (22)$$

Since the group velocity $d\omega/dK \rightarrow 0$ near the edges of allowed polariton bands ω_T and ω_L , Ω^{AB} then becomes strongly enhanced. The corresponding limit of Eq. (12) is

$$\gamma^{AB}(\omega_0, \mathbf{R})/\gamma_{\text{free}}^{AB}(\omega_0, \mathbf{R}) \simeq \epsilon_n^{3/2}(\omega_0) \left| 1 - \frac{\omega}{2} \frac{d}{d\omega} \ln \epsilon_n(\omega) \right|_{\omega_0}. \quad (23)$$

In the range of anomalous dispersion (but as long as $\text{Im}\epsilon_n \ll \text{Re}\epsilon_n$) $0 < \epsilon_n(\omega_0) < 1$, occurring near the plasma cutoff [Eq. (4)] or $\omega_0 \gtrsim \omega_L$ on the longitudinal polaritonic branch [Eq. (3)], $\gamma^{AB}(\omega_0, \mathbf{R})$ and the single-atom rate of emission $\gamma(\omega_0)$ will be suppressed (relative to free space) by a factor of at least $\epsilon_n(\omega_0)$. In the other extreme $\epsilon_n(\omega_0) \gg 1$ ($\omega_0 \lesssim \omega_T$ on transverse polaritonic branches) there will be strong enhancement of γ^{AB} and γ .

C. Allowed bands of photonic crystals

In the nearly free diffraction regime, we can retain in Eq. (9b) only the reciprocal-lattice vectors 0 and $2\pi/d$ and the corresponding Fourier coefficients C_0 and C_1 , which become near the edges of the allowed band^{27,30} $C_0 \simeq \pm C_1 \simeq \pm 2^{-1/2}$ (cosine or sine Bloch waves). Equation (9b) then reduces to

$$\Phi_{\omega_0}^{AB} \simeq \left[1 + \frac{\sin(\pi R/d)}{(\pi R/d)} \right] \left[1 \pm \frac{\sin(\pi r_B/d)}{(\pi r_B/d)} \right], \quad (24)$$

which ranges between 4 and 0 in the limit $R/d \ll 1$, depending on the Bloch wave. Thus, although $N_n(\omega_n)$ is enhanced near the band edge [Fig. 3(c)], diffraction can extinguish both γ^{AB} and Ω^{AB} if one of the atoms is located at a node of the field [Fig. 2(a)].

D. Band tails (pseudogaps)

We turn now to ω_0 in a pseudogap (band tail) of a nearly-periodic medium. A slight deviation from periodicity (by thermal or structural disorder) would only smooth out the DOM singularities at the edges of allowed bands, while keeping the DOM nearly vanishing in spectral regions that are forbidden in perfect crystals (Fig. 3). The resulting Ω^{AB} and γ^{AB} would then be subject to nearly the same R -independent suppression relative to their free-space values

$$\begin{aligned} \Omega^{AB}(\omega_0, \mathbf{R})/\Omega_{\text{free}}^{AB}(\omega_0, \mathbf{R}) &\simeq \gamma^{AB}(\omega_0, \mathbf{R})/\gamma_{\text{free}}^{AB}(\omega_0, \mathbf{R}) \\ &\simeq c^3 N_n(\omega_0)/\omega_0^2 \ll 1. \end{aligned} \quad (25)$$

IV. BAND GAPS

A. Nondissipative band gaps

In ideal photonic crystals or in nearly uniform media with negligible dissipation (absorption), the edge of a

band gap is a singularity of the DOM, where the real part of $dK/d\omega$ changes discontinuously and $N_n(\omega)$ vanishes abruptly.^{29,30} This immediately implies that within a bandgap

$$\gamma^{AB}(\omega_0, \mathbf{R}) \propto \gamma(\omega_0) \propto N_n(\omega_0) = 0. \quad (26)$$

The evaluation of Ω^{AB} calls for more care. Guidance is given by standard methods of electron or phonon band calculations.^{33–35} The frequency is expanded about the singularity ω_c (the lower or upper edge of the bandgap or the cutoff frequency in plasma or a waveguide):

$$\omega = \omega_c + b\kappa^2 + \dots, \quad (27)$$

where κ is the deviation from the wave vector of the band edge K_c ($=\pi/d$ in the lowest Bragg resonance) and the first-derivative term in the expansion vanishes at the singularity. Just below a cutoff frequency or the upper edge of a gap ω_c [Figs. 3(b) and 3(c)] this expansion corresponds to

$$N_n(\omega) \simeq \omega(\omega^2 - \omega_c^2)^{1/2} (2\omega_c b)^{-3/2} \Theta(\omega^2 - \omega_c^2), \quad (28)$$

where Θ is the Heaviside step function. A similar expression is obtained for ω_c at the lower edge of a gap.

Using this form of $N_n(\omega)$, Ω^{AB} can be evaluated for ω_0 just below a cutoff point ω_c on extending the integral in Eq. (13) over the domain $\infty > \omega > \omega_c$ and $-\omega_c > \omega > -\infty$ (allowing for the even parity of the integrand as in Sec. III A), excluding the forbidden band and its singular edges $\omega_c \geq \omega \geq -\omega_c$ by branch cuts and closing the contour by a circle of infinite radius [Fig. 4(b)]. The evaluation of Ω^{AB} for ω_0 in a gap between two allowed bands is similar, although the contour is more involved.

In both cases, the $\pm\omega_0$ residues contributing to the integral are determined by the analytic continuation of $N_n(\omega)$ [as given by Eq. (28)] and $[F(KR)\Phi^{AB}]_{\omega_n}$ into the gap. This yields

$$N_n(\pm\omega_0) = \kappa^2 \frac{\partial \kappa}{\partial \omega} = \pm i \omega_0 |\omega_0^2 - \omega_c^2|^{1/2} (2b\omega_c)^{-3/2}, \quad (29)$$

where κ is the imaginary part of the wave vector and ω_c denotes, in a gap between two bands, the edge closest to ω_0 . The analytically continued DOM is thus a purely imaginary, odd-symmetry function. The analytic continuation of $F(KR)\Phi^{AB}$ amounts to the replacement of the angular integral Eq. (9) by an integral over evanescent modes with complex wave vectors:

$$\begin{aligned} \int d\Omega_{\hat{\mathbf{k}}} (\hat{\boldsymbol{\mu}} \cdot \hat{\boldsymbol{\eta}}_\sigma)^2 \langle \Psi_\alpha^*(\mathbf{r}_A) \Psi_\alpha(\mathbf{r}_B) \rangle \\ \longrightarrow \int d\Omega_{\hat{\mathbf{k}}} (\hat{\boldsymbol{\mu}} \cdot \hat{\boldsymbol{\eta}}_\sigma)^2 \exp(i\mathbf{K} \cdot \mathbf{R} - |\boldsymbol{\kappa} \cdot \mathbf{R}|). \end{aligned}$$

The diffraction function Φ^{AB} is also strongly changed within the gap. Thus, in the nearly free diffraction regime, the Fourier coefficients at the center of a narrow gap and the corresponding Φ^{AB} are changed from their values in Eq. (24) to

$$C_0^* C_1 \simeq \pm i/2, \quad \Phi_{\pm\omega_0}^{AB} \simeq [1 + \sin(\pi R/d)/(\pi R/d)], \quad (30)$$

i.e., the $\pi/2$ phase shift in the Fourier coefficients elimi-

notes the location-dependent term.

This combination of analytically continued factors produces a remarkable change in the residue contributions to Eq. (13), as compared to Eq. (19), leading to

$$\begin{aligned} \Omega^{AB}(\omega_0, \mathbf{R}) / \Omega_{\text{free}}^{AB}(\omega_0, \mathbf{R}) \\ \simeq \Phi_{\pm\omega_0}^{AB} [c / (2\omega_c b)^{1/2}]^3 |1 - \omega_c^2 / \omega_0^2|^{1/2} \exp(-\kappa R)_{\omega_0} \\ \times F(KR)_{\omega_0} / G(\omega_0 R / c), \end{aligned} \quad (31a)$$

where we have used the imaginary antisymmetric form of $N_n(\pm\omega_0)$ in Eq. (29) to obtain [cf. Eqs. (8), (14), and (15)]

$$-i^2 [F(KR)_{+\omega_0} + F(KR)_{-\omega_0}] = F(KR)_{\omega_0}. \quad (31b)$$

Usually, $\kappa \lesssim K$ for ω_0 just within forbidden bands or in narrow gaps, where $K \simeq \pi/d$ at the first Bragg resonance in photonic crystals, or $K \simeq \omega_L \epsilon_0^{1/2} / c$ in a polaritonic bandgap²³ [Eq. (3)]. The predominant change in R dependence of RDDI within a gap is then that $G(KR)$, characterizing allowed bands, is replaced by $F(KR)$, because of the $\pi/2$ phase shift and symmetry change in the argument of $F(KR)_{\pm\omega_0}$.

The analytically continued DOM in Eq. (29), which has introduced these changes into $F(KR)_{\pm\omega_0}$, is responsible for interatomic coupling via *evanescent* modes that have wave vectors $i\kappa$ and are resonant with a virtual frequency whose imaginary part is $(\omega_0^2 - \omega_c^2)^{1/2}$. This is equivalent to coupling via *allowed* (normal) modes outside the gap which are shifted by $|\omega_0^2 - \omega_c^2|^{1/2}$ from resonance with the atomic frequency ω_0 . The resulting $\pi/2$ phase shift marks the interference between the emission of atom A and the *virtual* absorption (i.e., scattering resonance) of atom B , instead of the real absorption occurring in allowed bands. The consequence of the resonance being no longer real is that the R^{-3} -divergent limit of $G(KR)$ is “smoothed” out, becoming $F(KR)$ [compare Figs. 2(b) and 2(c)]. For typical intermolecular or interatomic separations R of a few Å and ω_0 in the optical

range, the factor $F(KR)_{\omega_0} / G(\omega_0 R / c)$ in Eq. (31a) can be as small as 10^{-9} or 10^{-10} , i.e., the suppression is extremely strong.

Additional suppression of the RDDI in a band gap can occur because the density of evanescent modes in Eq. (31) nearly vanishes for $\omega_0 \simeq \omega_c$, i.e., just inside the gap. This result is accurate for nearly uniform media, where the isotropic approximation (Sec. II B) is at its best. In fcc or bcc crystals, this approximation involves some smearing of the band edges, so that $|1 - \omega_0^2 / \omega_c^2|^{1/2}$ cannot be neglected, and should be considered comparable to the gap width normalized by the central frequency. Note that for ω_0 near the middle of a gap of appreciable width, the form of $N_n(\omega)$ in Eq. (29), which is obtained from a second-order expansion about ω_c , should be replaced by a more accurate analytic continuation.

B. Dissipative effects

Dissipation relaxes the sharp separation between allowed and forbidden bands, and leads to the mixing of effects pertaining to both types of dispersion. Near a band edge, the dispersion relation Eq. (27) is now modified into

$$(\omega + i\Gamma)^2 - \omega_c^2 \simeq 2\omega_c b \kappa^2, \quad (32)$$

where Γ is the absorption width associated with the imaginary part of the dielectric index.^{23,36}

The corresponding analytically continued DOM in the gap is then

$$\begin{aligned} N_n(\pm\omega_0) = \pm i \omega_0 (2\omega_c b)^{-3/2} |\omega_0^2 - (\omega_c^2 + \Gamma^2)|^{1/2} \\ \times \left[1 - \frac{4i\Gamma\omega_0}{|\omega_0^2 - (\omega_c^2 + \Gamma^2)|} \right]. \end{aligned} \quad (33)$$

The use of this complex DOM in the evaluation of RDDI, analogously to the nonabsorptive case adds another term to the latter result [Eq. (31)]:

$$\frac{\Omega^{AB}}{\Omega_{\text{free}}^{AB}} \simeq [c / (2\omega_c b)^{1/2}]^3 \frac{|1 - \omega_0^2 / \omega_c^2|^{1/2}}{G(\omega_0 R / c)} \Phi_{\pm\omega_0}^{AB} \left[\exp(-\kappa R)_{\omega_0} F(KR)_{\omega_0} + G(KR)_{\omega_0} \left[\frac{\Gamma\omega_0}{|\omega_0^2 - (\omega_c^2 + \Gamma^2)|} + \mathcal{O}(\Gamma/\omega_0) \right] \right]. \quad (34)$$

It is seen that the real part of the DOM restores the $G(KR)$ dependence characteristic of allowed bands. This means that the resonance broadening caused by dissipation permits resonant interatomic coupling in the gap via a “tail” of allowed (normal) modes. In order to keep RDDI small in the presence of dissipation one must minimize the prefactor of $G(KR)$ in Eq. (34), i.e., keep

$$\Gamma \ll |\omega_0 - \omega_c| \ll \omega_c. \quad (35)$$

V. DISCUSSION

The application of the formalism presented in Sec. II to allowed bands (Sec. III) and band gaps (Sec. IV) has

demonstrated that the RDDI as well as cooperative fluorescence of two-atom systems can be strongly enhanced or suppressed, to the extent of being essentially eliminated, by one of the following basic mechanisms.

(a) Dependence on location within a unit cell of a photonic crystal, i.e., sensitivity to the spatial variation of the field normal modes [Eqs. (9) and (24)]. In periodic structures composed of spheres, the location relative to the sphere center is also important [Eq. (10)].

(b) Dependence on the density of normal modes in an allowed band [Eqs. (22) and (23)] or a band tail [Eq. (25)], and on the analytic continuation of the DOM function into a band gap [Eq. (29)] which can be interpreted as the density of virtual modes. The $\pi/2$ phase shift and parity

change introduced by this analytic continuation into the integrand of RDDI leads to the elimination of the electrostatic R^{-3} -divergent limit of this interaction [Eq. (31)]. The RDDI is thereby strongly suppressed at interatomic separations that are small compared to the emission wavelength.

The ability to essentially eliminate the RDDI at interatomic separations characterizing quasimolecules (a few Å) would have far-reaching implications on their dissociative or collisional dynamics, spectroscopy and energy transfer properties.¹⁶ The symmetrized (ungerade) and antisymmetrized (gerade) states of a dimer:^{6,7}

$$|\pm\rangle = \{|e\rangle_A |g\rangle_B \pm |g\rangle_A |e\rangle_B\} 2^{-1/2}, \quad (36)$$

where e and g are the excited and ground atomic states, respectively, are energetically shifted by $\pm\Omega^{AB}$ from atomic resonance. The respective fluorescence rates are $\gamma^{AB} \approx 2\gamma$ (superradiance) and $\gamma - \gamma^{AB} \approx 0$ (subradiance). All these differences would nearly disappear in a band tail or a band gap.

If only atom A is excited prior to its collision with the ground-state atom B at $t=0$ (as in crossed-beam collisions), then the probability of atom B emerging from the collision at time t in an excited state is²⁶

$$\frac{1}{2}e^{-\gamma t} [\cosh(\gamma^{AB} t) - \cos(\Omega^{AB} t)].$$

In quasimolecular collisions occurring in allowed bands or free space, $|\Omega^{AB}| \gg \gamma^{AB} \approx \gamma$. The excitation probability of atom B then oscillates between 0 and 1 at the frequency Ω^{AB} due to photon exchange as long as $\gamma t \ll 1$, whereas for $\gamma t \gg 1$ this probability becomes trapped at the value of $\frac{1}{4}$. In contrast, within a gap, where $\gamma = \gamma^{AB} = 0$ and $0 \leq |\Omega^{AB}| \lesssim \gamma_{\text{free}}$, this excitation would oscillate indefinitely between 0 and 1, out of phase with that of atom A , at the very slow frequency $|\Omega^{AB}|$. These very slow oscillations would reflect the blocking of inter-

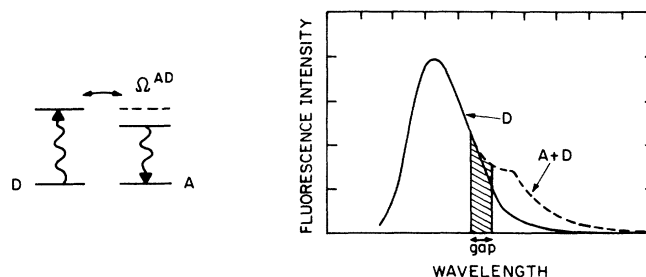


FIG. 5. The Förster-Dexter mechanism of excitation transfer from a donor (D) to an acceptor (A) via the RDDI. The fluorescence intensity of the donor (D) has a tail in the presence of an acceptor ($A+D$), which is suppressed when the overlap between the emission band of D and the absorption band of A is within a gap.

atomic photon exchange due to the absence of resonant normal modes, and their replacement by nonresonant (or virtual) modes.

The suppression of donor-acceptor energy transfer by RDDI (the Förster-Dexter mechanism⁴) in a band gap would change the fluorescence spectra of donor-acceptor complexes as shown schematically in Fig. 5. If the overlap between the emission band of the donor and the absorption band of the acceptor is within the gap, then a strong decrease of the fluorescence is anticipated in the emission band of the acceptor, solely due to RDDI suppression, even if the latter band is outside the gap.¹⁶

ACKNOWLEDGMENTS

Useful discussions are acknowledged with S. Alexander, A. Ben-Reuven, A. Genack, S. John, and A. Nitzan. This work has been supported in part by the U.S.-Israel Binational Scientific Foundation and by the M. Russell-Haas Career Development Fund.

¹D. P. Craig and T. Thirunamachandran, *Molecular Quantum Electrodynamics* (Academic, London, 1984).

²G. S. Agarwal, *Quantum Statistical Theories of Spontaneous Emission* (Springer-Verlag, Berlin, 1974).

³H. Margenau and N. R. Kestner, *Theory of Intermolecular Forces* (Pergamon, Oxford, 1971).

⁴Th. Förster, *Ann. Phys. (Leipzig)* **2**, 55 (1948); D. L. Dexter, *J. Chem. Phys.* **21**, 836 (1953).

⁵A. Kopystynska and L. Moi, *Phys. Rep.* **92**, 135 (1982).

⁶E. E. Nikitin, *Adv. Chem. Phys.* **28**, 317 (1975); E. E. Nikitin and S. Ya. Umanski, *Theory of Slow Atomic Collisions* (Springer, Berlin, 1984).

⁷G. Kurizki and A. Ben-Reuven, *Phys. Rev. A* **32**, 2560 (1985); **36**, 90 (1987); G. Kurizki, G. Hose, and A. Ben-Reuven, *ibid.* **38**, 6433 (1988).

⁸H. S. Freedhoff, *J. Phys. B* **20**, 285 (1987).

⁹K. H. Drexhage, in *Progress in Optics*, edited by E. Wolf (North-Holland, Amsterdam, 1974), Vol. 12, p. 165.

¹⁰R. R. Chance, A. Prock, and R. Silbey, *Adv. Chem. Phys.* **37**, 1 (1978).

¹¹R. G. Hulet, E. S. Hilfer, and D. Kleppner, *Phys. Rev. Lett.* **55**, 2137 (1985).

¹²P. W. Milonni and P. L. Knight, *Opt. Commun.* **9**, 119 (1973).

¹³G. Barton, *Proc. R. Soc. London Ser., A* **410**, 141 (1987); *Phys. Scr.* **T21**, 11 (1988).

¹⁴S. Druger, S. Arnold, and L. M. Folan, *J. Chem. Phys.* **87**, 2649 (1987).

¹⁵P. T. Leung and K. Young, *J. Chem. Phys.* **90**, 2894 (1988).

¹⁶G. Kurizki and A. Genack, *Phys. Rev. Lett.* **61**, 2269 (1988).

¹⁷E. Yablonovitch, *Phys. Rev. Lett.* **58**, 2059 (1987).

¹⁸S. John, *Phys. Rev. Lett.* **58**, 2486 (1987); *Comments Cond. Matter Phys.* **14**, 193 (1988).

¹⁹S. John and J. Wang, *Phys. Rev. Lett.* **64**, 2418 (1990).

²⁰E. Yablonovitch and T. Gmitter, *Phys. Rev. Lett.* **63**, 1950 (1989).

²¹G. Kurizki, in *Coherence and Quantum Optics VI*, edited by J. H. Eberly, L. Mandel, and E. Wolf (Plenum, New York, 1990), p. 631.

²²J. Knoester and S. Mukamel, *Phys. Rev. A* **40**, 7065 (1989).

²³D. L. Mills and E. Burstein, *Rep. Prog. Phys.* **37**, 817 (1974).

²⁴R. Claus, L. Merten, and J. Brandmüller, *Light Scattering by Phonon Polaritons* (Springer-Verlag, Berlin, 1975).

²⁵J. B. Grun, B. Hönerlage, and R. Levy, *Solid State Commun.* **46**, 51 (1983); J. Y. Bigot and B. Hönerlage, *Phys. Status Soli-*

- di B **121**, 649 (1984). See also H. Haug and S. Schmitt-Rink, *Prog. Quantum Electron.* **9**, 3 (1984).
- ²⁶R. H. Lehmberg, *Phys. Rev. A* **2**, 883, 889 (1970).
- ²⁷J. C. Slater, *Rev. Mod. Phys.* **30**, 197 (1958); See also G. Borrmann, *Trends in Atomic Physics*, edited by O. R. Frisch (Interscience, New York, 1959).
- ²⁸P. W. Milonni and P. L. Knight, *Phys. Rev. A* **10**, 1096 (1974).
- ²⁹J. M. Ziman, *Principles of the Theory of Solids* (Cambridge University Press, Cambridge, 1965).
- ³⁰W. Jones and N. H. March, *Theoretical Solid State Physics* (Dover, New York, 1985), Vol. 1.
- ³¹H. Winston, *J. Chem. Phys.* **19**, 156 (1951).
- ³²S. John and R. Rangarajan, *Phys. Rev. B* **38**, 10101 (1988).
- ³³H. J. Goldsmid, *Problems in Solid State Physics* (Academic, New York, 1968), Chap. 15.
- ³⁴J. C. Phillips, in *Solid State Physics*, edited by F. Seitz and D. Turnbull (Academic, New York, 1966), Vol. 18.
- ³⁵F. Stern, in *Solid State Physics*, edited by F. Seitz and D. Turnbull (Academic, New York, 1963), Vol. 15.
- ³⁶R. Loudon, *J. Phys. A* **3**, 233 (1970).